



# Relaxation of silica glass surfaces before and after stress modification in a wet and dry atmosphere: molecular dynamics simulations

Edmund B. Webb III, Stephen H. Garofalini \*

*Department of Ceramic and Materials Engineering, Interfacial Molecular Science Laboratory, Rutgers University, Piscataway, NJ 08854, USA*

Received 10 March 1997; revised 8 December 1997

---

## Abstract

Previous molecular dynamics simulations have shown that compression of silica glass surfaces occurs upon formation of an interface with a model crystal and that a structural change caused by this process is retained after glass and crystal are separated. The remnant structural modification caused by this stress was an increase in the concentration of siloxane bond angles less than  $150^\circ$  in the near surface region of the glass. It was expected that the structural modification associated with interface formation and separation could represent an increase in the concentration of less stable siloxane bonds, particularly in the presence of water molecules. It was also recognized that a decreased stability could indicate greater reactivity with water molecules. Thus, water reaction on silica surfaces was simulated before and after stress modification and the subsequent structural relaxations in the glass surface were observed. Decreased stability, represented by a greater number of bond ruptures, existed after interface formation and removal. These bond ruptures were Si–O bonds breaking and reforming siloxane bonds with an angle nearer the average and also Si–O bonds breaking to react with water forming silanols. A greater number of silanols formed after interface formation and removal than before, demonstrating a greater reactivity with water after interface formation and separation. © 1998 Elsevier Science B.V. All rights reserved.

---

## 1. Introduction

Bonding to or reacting with silica glass surfaces is of interest to many industries such as microelectronics and fiber optics. An attempt to understand bonding with these surfaces must begin with a correct description of the surface properties. Because the state of a silica glass surface is determined by ther-

mal history and processing conditions, a variety of states is to be expected [1]. Consequently, many experimental studies have been performed and the properties of silica surfaces formed under various conditions along with generalized surface features have been established [2–17]. In particular an average of four silanols per  $\text{nm}^2$  exists on the surface [9]. For many reactive adsorbates, surface silanols are sites of initial reaction with silica glass surfaces. An example is reaction with water in which silanols serve as initial sites for water interaction via hydrogen bonding increasing subsequent reactions with the

---

\* Corresponding author. Tel.: +1-908 445 4655; fax: +1-908 445 4655; e-mail: shg@rutile.rutgers.edu.

glass structure. Such progressive reaction with water is known to have deleterious effects on glass strength and durability [18]. Therefore, factors determining silanol creation and concentration are pertinent to engineering applications for silica glass.

Formation of interfaces with silica glass through simulated gas phase deposition of model metal atoms was previously shown to compress the glass surface  $\sim 1$  Å [19]. A result of this compression by interface formation was a shift in the structural statistics of the glass surface. Specifically, there was an observed increase in siloxane bond angles less than  $\sim 150^\circ$  in the top 6 Å of the glass. A similar result was seen when a model crystalline metal was brought in contact with silica glass to form an interface at room temperature [20]. That work demonstrated that there is a few angstrom compression of the glass surface upon interface formation which is localized to the top 10 Å of the glass. The glass surface compression was the same in unpublished simulations using a glass four times larger in the direction normal to the interface. The compression observed is not system or strain size dependent but, rather, is a surface effect inherent to interface formation with silica glass. The effect of this compression, in all system sizes studied, is a similar shift in siloxane bond angles to a higher concentration of angles less than  $\sim 150^\circ$ . In addition, previous simulations have shown that a part of the increase in small siloxane bond angles remained when the crystal was separated from the glass [20].

These sites may be of interest as there is a variety of work showing preferential water interaction with siloxane bonds forming angles in the region of  $135^\circ$ . Geometric constraints provide the three member ring which has siloxane bond angles in the range of  $135^\circ$  and experiments have shown these species to be more reactive with water [14]. Molecular orbital calculations on silicate molecules have demonstrated that small siloxane bond angles are accompanied by elongated siloxane bonds. These bonds are, thus, larger in energy and would be expected to be less stable or more reactive [21]. Previous MD simulations of water reacting with silica surfaces [22] give evidence to this preference as well. As such, sites of smaller siloxane bond angles ( $\sim 135^\circ$ ) may serve as initial hydroxylation sites on a silica surface. These observations indicate that the compression of the

silica surface that occurs upon interface formation may result in a less stable surface structure. This decreased stability could mean that a surface which is more reactive with water has been created. This reactive surface is relevant if water is present at some interface upon formation as the state of the silica surface could change after the interface is formed. The simulations showing a remnant increase in smaller siloxane bond angles after removal of the model crystal are also relevant. These possibly indicate that contact with glass surfaces inherent to glass processing procedures could decrease the stability of the surface structure. Again, decreased stability could indicate increased reactivity with water. Since silanol sites are often initial reaction sites for other adsorbates, an increase in reactivity with water would most probably produce a generally more reactive surface [9].

Herein simulations of water reacting on glass surfaces both before and after stress modification are presented. The stress modification was achieved by a low temperature (300 K) interface formation and removal with a model crystal. Subsequent relaxation of the surfaces in the presence of water is analyzed with emphasis placed on identifying differences in reactions before and after stress modification. Much previous MD simulation work investigating water reactions on silica surfaces has been performed using the same potential model used here [22–24]. As such, the present work does not serve as a complete description of this process and the interested reader is directed to the references. Rather, an attempt is made here to establish whether differences in the process exist due to the interface formation and removal.

## 2. Computational procedure

All interactions present in these simulations were governed by the multibody potential developed by Feuston and Garofalini [25]. This potential has been utilized previously to study the relaxation of silica surfaces in the presence of water [23,24]. Briefly, the potential consists of a two-body and three-body term:

$$V(R_i) = \sum_{j \neq i} V_{ij}^{(2)} + \sum_{j \neq i} \sum_{k \neq j \neq i} V_{jik}^{(3)} \quad (1)$$

where  $R_i = (r_1, r_2, \dots, r_n)$  for an  $n$ -atom system and the position of the  $i$ th atom is given by  $r_i$ . The two-body term is given by:

$$V_{ij}^{(2)} = A_{ij} \exp\left(\frac{-r_{ij}}{\rho_{ij}}\right) + \frac{Z_i Z_j e^2}{r_{ij}} \operatorname{erfc}\left(\frac{r_{ij}}{\beta_{ij}}\right) \quad (2)$$

where  $r_{ij} = |r_i - r_j|$ ,  $Z_i$  = the formal ionic charge on atom  $i$  and  $A_{ij}$ ,  $\rho_{ij}$ , and  $\beta_{ij}$  are adjustable pair parameters. The three-body term is:

$$V_{ijk}^{(3)} = \left\{ \lambda_{jik} \exp\left[\frac{\gamma_{ij}}{r_{ij} - r_{ij}^0} + \frac{\gamma_{ik}}{r_{ik} - r_{ik}^0}\right] \Omega_{jik} \right\} \quad (3)$$

when  $r_{ij} < r_{ij}^0$  and  $r_{ik} < r_{ik}^0$   
= 0 otherwise

where  $\gamma_{ij}$  is an adjustable pair parameter controlling the radial strength,  $\lambda_{jik}$  is an adjustable three-body parameter controlling the overall strength of the triplet term, and  $\Omega_{jik}$ , the angular term, is a function of  $\theta_{jik}$ , the angle formed by atoms  $i$ ,  $j$ , and  $k$  with atom  $i$  at the vertex. In this work, the following angular term was utilized:

$$\Omega_{jik} = (\cos \theta_{jik} - \cos \theta_{jik}^c)^2 \quad (4)$$

where  $\theta_{jik}^c$  is the equilibrium bond angle. The parameters utilized for the two-body and three-body terms are given in Tables 1 and 2, respectively; the respective ionic charges utilized for Si, O, and H were +4, -2, and +1. For all interactions involving hydrogen, additional terms were added to the two-body part of the potential curve. These have the form:

$$V_{H-X} = \frac{a_{HX}}{\{1 + \exp(b_{HX}(r_{HX} - c_{HX}))\}} \quad (5)$$

where X is either Si, O, or H and  $a_{HX}$ ,  $b_{HX}$ , and  $c_{HX}$  are adjustable pair parameters. Addition of such terms allows the shape of the pair potential to be modified at specific separation distances. For each term added, a different position on the curve can be modified allowing for a representation of both inter- and intramolecular interactions on a single continuous function [26]. One such term was added to the Si-H curve, two to the H-H curve, and three to the O-H curve. The parameters for these terms are presented in Table 3. Discussion of the respective

Table 1  
Parameters in the two-body term of the potential (Eq. (2))

Atom pair	$A_{ij} (\times 10^{-8} \text{ ergs})$	$\beta_{ij} (\text{\AA})$	$\rho_{ij} (\text{\AA})$
Si-Si	0.18770	2.29	0.29
Si-O	0.29620	2.34	0.29
Si-H	0.00690	2.31	0.29
O-O	0.07250	2.34	0.29
O-H	0.03984	2.26	0.29
H-H	0.00340	2.10	0.35

parameterization of all parts of the potential equation can be found elsewhere [27]. It should be pointed out that the parameterization used was determined by comparison of MD simulated structures and energetics for H<sub>2</sub>O and H<sub>4</sub>SiO<sub>4</sub> groups with similar statistics from experiment and ab initio calculations [28–32]. This parameterization has been successfully used previously to simulate silica surface formation in the presence of water, initial network formation in sol-gel processes, and subsequent network growth or polymerization [24,27,33–35].

The MD calculations were done using a fifth-order Nordsieck-Gear predictor/corrector algorithm [36] to integrate Newton's classical equations of motion. The simulations were performed in the micro-canonical ensemble (N-V-E). The cutoff distance for considering atom pairs in the two-body potential calculation was taken to be 0.55 nm for all simulations performed. The time step utilized for all simulations was  $1 \times 10^{-16}$  s (0.1 fs); this time step was utilized due to the presence of hydrogen.

Table 2  
Parameters in the three-body term (Eqs. (3) and (4))

	O-Si-O	Si-O-Si	Si-O-H	H-O-H
$\lambda (\times 10^{-11} \text{ ergs})$	19.0	0.3	5.0	35.0
$\gamma (\text{\AA})$				
Si-O	2.8			
O-Si		2.0	2.0	
O-H			1.2	1.3
$r^0 (\text{\AA})$				
Si-O	3.0			
O-Si		2.6	2.6	
O-H			1.5	1.6
$\theta^c (\text{degrees})$	109.5	109.5	109.5	104.5

Table 3  
Parameters for additional hydrogen pair terms (Eq. (5))

Atom pair	$a$ ( $\times 10^{-12}$ ergs)	$b$ ( $\text{\AA}^{-1}$ )	$c$ ( $\text{\AA}$ )
Si–H	–4.6542	6.0	2.20
H–H	–5.2793	6.0	1.51
	+0.3473	2.0	2.42
O–H	–2.0840	15.0	1.05
	+7.6412	3.2	1.50
	–0.8336	5.0	2.00

Creation of the two glass surfaces studied here was described in a previous publication [20]. The glass surfaces were stress-modified by bringing them into compressive contact with a model metal crystal and then removing the crystal. A description of the approach and withdrawal of the model crystal to the silica surfaces was previously presented, as was the effect of this process on the glass surface structures [20].

In the present work, the crystal was separated from the glass surfaces a sufficient distance so that there was no more interaction and then removed from the simulation box. As such there were two surface states from each glass to study water reactions on: before and after the crystal had been approached and pulled off (that is, before and after stress modification). Results presented in Ref. [20] motivated the comparison between water deposition on the glass surfaces before and after stress modification. Using two glasses, four deposition and reaction simulations were performed. The deposition and reaction procedure used for all four surface states is presented below; a schematic time line of the procedure is presented in Fig. 1. Whenever thermal equilibration was performed it was done by appropriately scaling the velocity of all mobile atoms every 20 time steps.

Each surface was first run for 10 ps at 300 K with thermal equilibration occurring during the first 5 ps. The next 30 ps were used for deposition of the water molecules above the surface. The method of placing a given water molecule was the same as described by Feuston and Garofalini [23]. The deposition process here can be broken up into six equivalent 5 ps parts. At the start of each part, an attempt to place 10 water molecules above the surface was made. During the next 5 ps, thermal equilibration to 300 K was performed for 2.5 ps, then the system was allowed to

evolve unperturbed for an additional 2.5 ps. With six such parts, a maximum of 60 water molecules could have been placed into the volume above a glass surface. However, there were restrictions on how close a water molecule could be placed to already existing atoms and a limited number of attempts were made to place each molecule. Thus, for glass 1 before and after stress modification, 37 water molecules of the 60 possible were placed above the surfaces. For glass 2 before and after stress modification, 38 water molecules were placed. The dimensions of the simulation box parallel to the surfaces were 1.97 nm by 1.95 nm. The reflecting boundary that defined the top of the simulation box was  $\sim 0.4$  nm above the termination of the glass surface. As such, the number of water molecules deposited above each surface resulted in a water film with a density  $\sim 75\%$  of liquid water. While the exact number of molecules deposited is different for the glass 1 surfaces compared to the glass 2 surfaces, the achieved density is nearly equivalent. Furthermore, the intent here is to compare, for a given surface, the relaxation

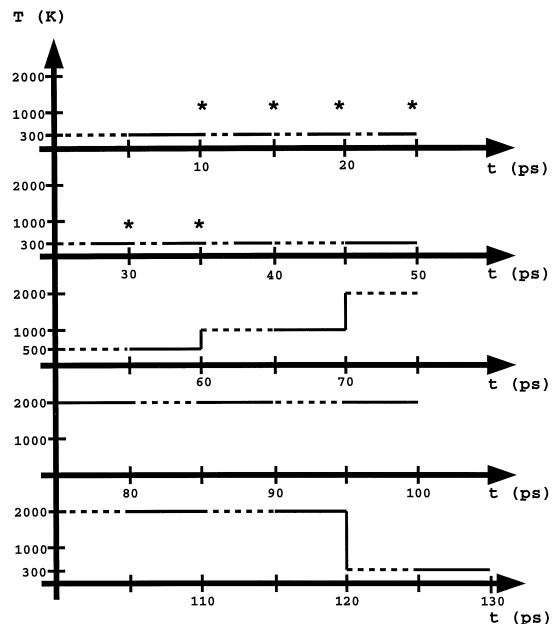


Fig. 1. Schematic time line showing procedure for water deposition and reaction. Broken line segments indicate thermal equilibration periods; asterisks indicate points in time where water molecules were added to the system. The schematic is the same for the dry anneal procedure except that no attempts to place water molecules were made.

observed in the presence of water before and after stress modification. Since for each surface, the number of water molecules deposited is the same before and after, such a comparison can be made.

After water deposition, surfaces were run for another 10 ps at 300 K with no deposition and thermal equilibration was performed for the first 5 ps. No relaxation of the silica surfaces was seen to occur at this low temperature despite the presence of water. Relaxation of the silica surfaces was then promoted by increasing the temperature. This increase is often done in simulations of reactions with water in order to reduce the total simulation time. In addition, melting points of silica crystals simulated with the potentials used here are higher than what is observed experimentally.

Elevated temperature relaxation was performed as follows. After deposition and subsequent equilibration at 300 K, each surface was run for 10 ps thermally equilibrating to 500 K for the first half of the run. The surfaces were then run for 10 ps with the temperature being equilibrated to 1000 K for the first 5 ps. For the next 50 ps the surfaces were run at a temperature of 2000 K. This was maintained by periodic thermal equilibration; every 10 ps, the system temperature was equilibrated to 2000 K for 5 ps. Finally, surfaces were quenched back to 300 K by thermal equilibration for 5 ps and then allowed to run unperturbed for an additional 5 ps.

Structural statistics from the non-equilibration segments of the 300 K run before water deposition and the final 300 K run after water reaction were generated. Features of primary interest were the siloxane bond angles present in the glass surfaces so siloxane bond angle distributions were created. To make all the curves surface specific, a set number of central oxygens were included in each analysis. The 50% of the mobile oxygen atoms closest to the surface were considered and, on all glass surface states analyzed, that corresponded to a depth of  $\sim 0.65$  nm. To better compare distributions before and after the simulated water reaction, delta distributions were created by subtracting the curve before water deposition from the curve after water reaction. For reasons outlined in Section 1, attention was primarily placed on siloxane bond sites that fell between  $120^\circ$  and  $140^\circ$ . Because the y-axis of all curves presented shows number of siloxane bond

angles, integration of the delta curves from  $120^\circ$  to  $140^\circ$  and division of the resultant number by the surface area simulated gives the change in concentration of these siloxane bond angle sites.

After water reaction, other structural features of interest were the silanol concentrations on the glass surfaces before and after stress modification. To calculate this value, both non-bridging oxygens (NBOs) and actual hydroxyl sites were counted since it is expected that with sufficient simulation time all NBOs would hydroxylate. Only the top 0.6 nm of the surfaces were considered and the cut-offs for oxygen/silicon and oxygen/hydrogen bonding were 0.2 nm and 0.11 nm, respectively.

One issue that arose due to the described procedure is whether the observed relaxation mechanisms could be caused solely by the elevated temperatures employed. As such, all four surface states (glass 1 and 2, before and after stress modification) were subjected to the same temperature cycle as described above only without any water deposited above them. Similar structural statistics were then generated from those simulations and used to ascertain the part of the relaxation attributable to the presence of water.

### 3. Results

Figs. 2–6 are siloxane bond angle distributions generated from the simulations using glass 1. Similar

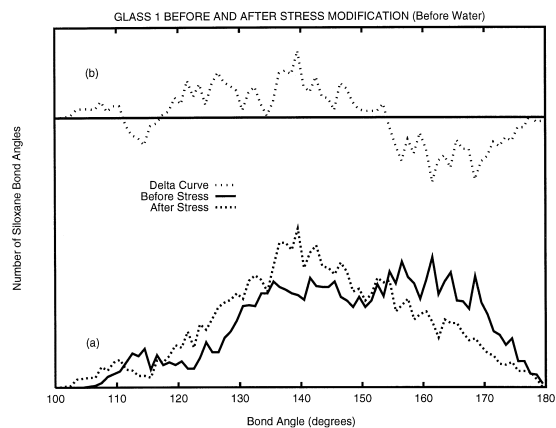


Fig. 2. (a) Siloxane bond angle distributions for glass 1 prior to reaction with water, before and after stress modification. (b) Delta curve formed by subtracting before stress modification curve in (a) from the after curve.

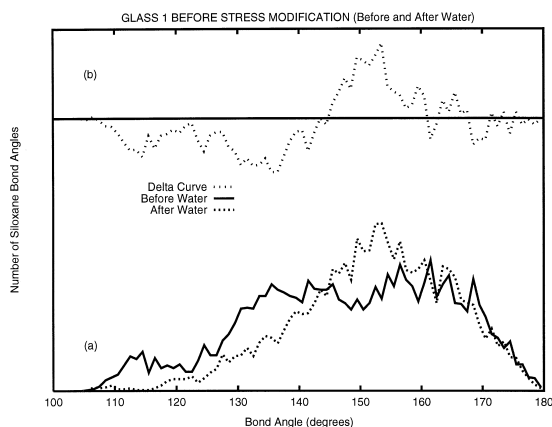


Fig. 3. (a) Siloxane bond angle distributions for glass 1 prior to stress modification, before and after reaction with water. (b) Delta curve formed by subtracting the before water reaction curve in (a) from the after curve.

data were generated and are discussed for glass 2 but, since the results were qualitatively the same, only the first of those figures is presented to avoid redundancy. The same analysis was performed on the two glasses; results from glass 1 are presented first followed by those from glass 2.

The structural change of interest that occurred upon stress modification is presented in Fig. 2a. Therein are the siloxane bond angle distributions for glass 1 before and after stress modification, but prior to reaction with water. Analysis of these curves shows the net increase in concentration of bond angles less than  $\sim 150^\circ$  along with a net decrease in those greater than  $150^\circ$ . Another description of the change in siloxane bond angle distribution upon stress modification is presented in Fig. 2b. This is the delta distribution created by subtracting the before stress curve from the after stress curve. Analyzing the delta curve, the trends already discussed are again evident as the curve is positive in the range less than  $150^\circ$  and negative in the region of larger bond angles. Integration of the delta distribution from  $120^\circ$  to  $140^\circ$  gives the result that  $\sim 3.6$  net sites per  $\text{nm}^2$  are formed in this angular range during stress modification. This result and the results of all integrations performed are collected in Table 4.

It should be pointed out that the response of the glass to stress modification is not simply to add sites in this angular range; rather, many bond angles

increase and decrease but the net result is the observed increase in small bond angles. In addition, only a small degree of bond rupture occurred during the stress modification, most of which was at surface defect sites. Thus, the bond angle distribution shift is largely made up by compression of preexisting siloxane bonds.

Fig. 3a and b and Fig. 4a and b are presented to show the effect of water reaction on the two surface states for glass 1. Fig. 3a shows two siloxane bond angle distributions for the glass 1 surface before stress modification; one curve is for before water reaction and the other is for after. Upon reaction with water, there was a decrease in the concentration of siloxane bond angle sites in the range of  $120^\circ$  to  $140^\circ$ . Integration of the delta curve in Fig. 3b from  $120^\circ$  to  $140^\circ$  shows that  $\sim 3.4$  sites per  $\text{nm}^2$  were removed during reaction with water; this is also shown in Table 4. Previous MD simulations have demonstrated this instability of siloxane bonds forming an angle in the range of  $120^\circ$  to  $140^\circ$  when in the presence of water [22]. These same data were generated for the glass 1 surface after stress modification and the results are in Fig. 4a and b. A similar integration of the delta curve in Fig. 4b shows  $\sim 8.1$  sites per  $\text{nm}^2$  removed from the angular range of interest during reaction with water. These data demonstrate that there were  $\sim 4.7$  more sites per  $\text{nm}^2$  removed from the angular range of interest after

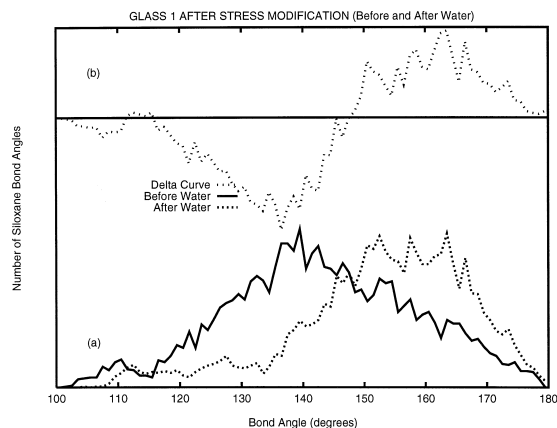


Fig. 4. (a) Siloxane bond angle distributions for glass 1 following stress modification, before and after reaction with water. (b) Delta curve formed by subtracting the before water reaction curve in (a) from the after curve.

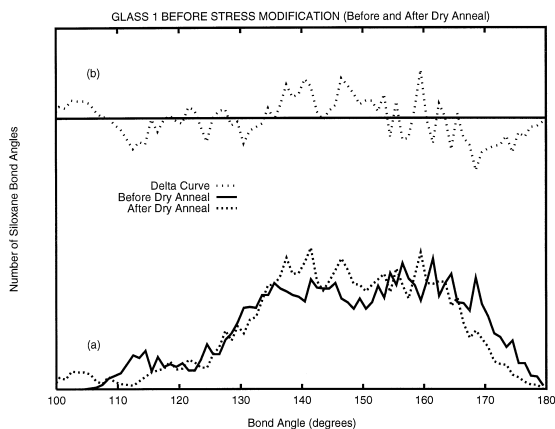


Fig. 5. (a) Siloxane bond angle distributions for glass 1 prior to stress modification, before and after dry anneal. (b) Delta curve formed by subtracting the before dry anneal curve in (a) from the after curve.

stress modification. This indicates that the net increase in sites produced by stress modification was removed during reaction with water. It might be expected that the only difference between the two surface states would be due to the net sites introduced by stress modification. If this were the case, then the difference in the number of sites removed during water reaction would equal the number of sites introduced by the stress modification ( $\sim 3.6$  per  $\text{nm}^2$ ). However, this difference was  $\sim 4.7$  sites per  $\text{nm}^2$ . The difference between these two values gives evidence that stress modification has a greater effect on the glass surface than indicated by the net sites formed. While the net sites formed are seen to be unstable in the presence of water, there is also an additional instability introduced shown by the additional  $\sim 1.1$  sites per  $\text{nm}^2$  that are unstable in the presence of water after stress modification.

It was necessary to establish that the greater instability of this region in the presence of water could be associated with greater reactivity. One direct method of showing this was to calculate the silanol concentration for the surfaces before and after stress modification. Generally, one would suspect a more reactive surface structure to have a greater hydroxyl concentration. For glass 1, the surface hydroxyl concentrations obtained for surfaces exposed to water before and after stress modification were 4.9 per  $\text{nm}^2$  and 6.2 per  $\text{nm}^2$ , respectively. These num-

bers indicate greater hydroxylation after stress modification. Not all bonds that ruptured became NBOs or silanols; some simply reformed network bonds at an angle outside the range of interest (i.e., nearer the average). While the behavior of these sites does not contribute to a higher silanol concentration, it does still indicate greater instability in the presence of water.

The final point that needs to be established is whether the relaxation of the unstable sites was facilitated by the presence of water. As was stated in Section 2, the elevated temperature that was employed to promote glass reactions with water may have induced structural relaxations independent of the water. As such, the temperature cycle employed in the presence of water was repeated on all surface states but without water present (for clarity, this will be called a dry anneal). Fig. 5a shows siloxane bond angle distributions for the glass 1 surface before stress modification, for both before and after the dry anneal. Integration of the delta curve in Fig. 5b from  $120^\circ$  to  $140^\circ$  shows that an increase in the number of sites in this range occurred during dry annealing; the increase was  $\sim 0.4$  sites per  $\text{nm}^2$ . During the reaction with water, sites were removed from this range and this is evidence that the removal of those sites was a consequence of the water and not a result of thermal agitation. As was already pointed out, not all of the sites that relax in the presence of water do so

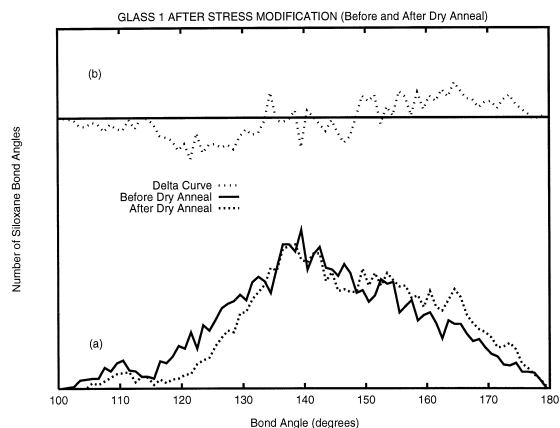


Fig. 6. (a) Siloxane bond angle distributions for glass 1 following stress modification, before and after dry anneal. (b) Delta curve formed by subtracting the before dry anneal curve in (a) from the after curve.

Table 4  
Results of delta curve integrations from 120° to 140° (in sites per nm<sup>2</sup>)

Delta curve	Glass 1	Glass 2
Before and after stress modification (before water)	+3.6	+3.9
Before stress modification (before and after water)	−3.4	−1.8
After stress modification (before and after water)	−8.1	−6.1
Before stress modification (before and after dry anneal)	+0.4	+0.7
After stress modification (before and after dry anneal)	−1.9	−2.1

by reacting with water. However, the dry anneal results indicate that the instability of these sites was increased by the presence of water. Fig. 6a and b show the effect of the dry anneal on the glass 1 surface after stress modification. A similar integration of the delta curve in Fig. 6b shows that  $\sim 1.9$  sites per nm<sup>2</sup> were removed from the angular range of interest during the dry anneal. Recall that, upon reaction with water,  $\sim 8.1$  sites per nm<sup>2</sup> were removed from this range and this number demonstrated that  $\sim 4.7$  additional unstable sites per nm<sup>2</sup> existed on the glass 1 surface after stress modification. Even if the  $\sim 1.9$  sites per nm<sup>2</sup> that are removed by dry annealing are subtracted from the  $\sim 4.7$  additional unstable sites, there are still  $\sim 2.8$  additional sites per nm<sup>2</sup> after stress modification that are thermally stable in a dry atmosphere but unstable in the presence of water. This result is evidence that the stress modification of glass 1 did produce a structure that was more unstable in the presence of water and that this additional instability could not be removed by thermal stress alone.

The same analysis presented above was done on glass 2 which possessed different surface structural statistics than glass 1 upon formation. Evidence of these differences is given by the siloxane bond angle distributions for glass 1 and glass 2 in Fig. 2a and Fig. 7a, respectively. Fig. 7a and b are the only figures presented for glass 2 since the qualitative results of the analyses are the same for glass 2 as for glass 1. The same integrations described for glass 1 were done on the glass 2 data and those results are tabulated in Table 4.

Comparison of Fig. 7a for glass 2 and Fig. 2a for glass 1 shows that the qualitative result of stress modification is the same for both glasses: an increase in concentration of angles less than  $\sim 150^\circ$  with an accompanying decrease at larger angles. Integration

of the delta curve in Fig. 7b from 120° to 140° shows a net increase upon stress modification of  $\sim 3.9$  sites per nm<sup>2</sup> (compared to  $\sim 3.6$  for glass 1). Similar to glass 1, most of the change in the bond angle distribution was caused by compression of preexisting siloxane bond angles rather than bond breaking.

As shown in Table 4, water reaction on the glass 2 surface before stress modification removes  $\sim 1.8$  sites per nm<sup>2</sup>. After stress modification,  $\sim 6.1$  sites per nm<sup>2</sup> were removed from the angular range of interest in the presence of water. The numbers show that an additional  $\sim 4.3$  sites per nm<sup>2</sup> existed on the glass 2 surface after stress modification that were unstable in the presence of water (for glass 1 this number was  $\sim 4.7$ ). Furthermore, as was also the case with glass 1, the number of additional unstable sites is greater than the number of sites introduced by the stress modification. Again, this is evidence that the effect of stress modification on the glass

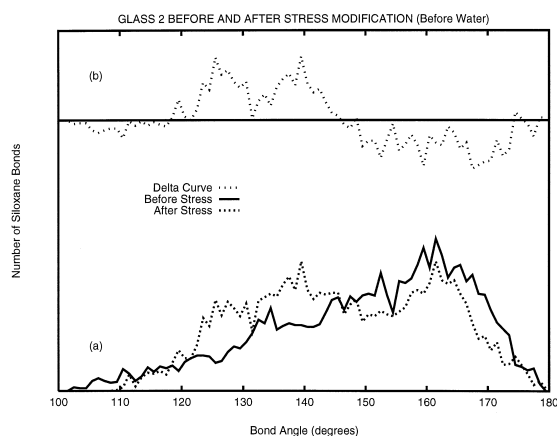


Fig. 7. (a) and (b) same as Fig. 2 (a) and (b) but with data for glass 2.

surface stability is at least somewhat more far reaching than what is indicated by the number of sites formed by the stress.

As was done previously for glass 1, the silanol concentrations were calculated on the glass 2 surfaces before and after stress modification. Before stress modification, hydroxylation resulted in 4.4 silanols per  $\text{nm}^2$  while afterward it resulted in 6.2 silanols per  $\text{nm}^2$ . For comparison, these numbers for the glass 1 surface before and after stress modification were 4.9 and 6.2, respectively. This result is taken as further evidence that the greater instability of the glass surfaces after stress modification is associated with higher reactivity in the presence of an adsorbate such as water.

Heating glass 2 in the absence of water produced similar results to those obtained from glass 1. Table 4 shows that, before stress modification,  $\sim 0.7$  sites per  $\text{nm}^2$  were added during the dry anneal. Since sites were removed from this range in the presence of water, this is evidence that the sites removed were thermally stable in a dry atmosphere but unstable in the presence of an adsorbate. After stress modification, the dry anneal removed  $\sim 2.1$  sites per  $\text{nm}^2$  from the angular range of interest. Recall that after stress modification  $\sim 6.1$  sites were removed from this range in the presence of water. Data showed that, in the presence of water, there were  $\sim 4.3$  additional unstable sites per  $\text{nm}^2$  after stress modification. If  $\sim 2.1$  of these additional sites were thermally unstable, that leaves  $\sim 2.2$  sites per  $\text{nm}^2$  introduced by stress modification that are thermally stable in a dry atmosphere yet unstable in the presence of water. For glass 1, this number was  $\sim 2.8$  sites per  $\text{nm}^2$ .

#### 4. Discussion

While the primary purpose of the data presented is to compare surface behavior before and after the stress modification, some general observations can be made about all the siloxane bond angle distributions. The fact that the curves are obtained from a surface specific region is exemplified by their shapes. In all figures presented, the siloxane bond angle distributions differ from those obtained using simu-

lated bulk silica glass or from experimental data. This difference is because the ones herein show features caused by specific surface structures while experimental curves are averaged over an overwhelmingly dominant bulk contribution. One feature present in most of the bond angle distributions is a contribution at angles  $< 120^\circ$ . This angular region is often associated with defect structures such as two-member rings and over-coordinated silicons. In the data presented here, those species do account for the contributions to angles  $< 120^\circ$  and it was expected that these larger energy structures would be the first to be removed during either reaction with water or a dry anneal. In some cases, removal was observed but because of the short simulation durations not all of these surface defect structures were removed. It is expected, and has been observed previously [22], that these species would eventually be removed if the simulation times were extended.

Comparison of the before stress modification curves in Fig. 2a and Fig. 7a for glass 1 and 2, respectively, provides a view of the glass surfaces in their 'as formed' states. The distinctly different shapes indicate that surface structures of the two glasses differed. As discussed elsewhere [20], these two glasses were subjected to different simulated thermal histories during formation and so differences in the surface statistics are to be expected. Despite different surface statistics in their as formed states, the trends displayed by these two glasses were the same and the quantitative results were similar. After stress modification, both glasses showed an increase in sites that were thermally stable in a dry atmosphere but unstable in the presence of water. At the temperature used here. Furthermore, both glasses showed a larger concentration of silanols after stress modification and, again, the increase was similar for the two glass surfaces.

The results presented are pertinent for a number of reasons. The stress modification which altered the surface structure involved a few angstrom compression of the silica surface. Furthermore, previous work showed that similar compression results when an interface is formed with silica glasses by a simulated gas phase atom deposition [19]. In general, previous results indicate that interface formation with silica glasses creates a region in the glass near the interface that is in compression. Previous simulations

also show that, in instances where the interface formed is then removed, some of this compression of the near surface region remains [20].

The present results demonstrate that the remnant surface structure is thermally stable but produces sites which are unstable in the presence of water at the temperature used here. Furthermore, this remnant structure is seen to result in larger silanol concentrations indicating a greater reactivity. Many physical processes involving silica glasses could induce such surface alterations. Film formation via deposition, wafer bonding, and catalytic particle support are instances where the slight compression of the glass surface simulated here might be expected. In addition, contact with glass surfaces inherent to processing of glass samples could result in the low levels of compression that were observed here. The present simulations demonstrate that the stability of these compressed regions of the glass may be lessened in the presence of water. The surface state of a glass may be more reactive after a compressive event even if the compression is localized to the near surface region of the glass. The possibility also exists that, for interfaces involving silica glass, the structure of the interfacial region could shift at temperatures below the glass transition region. These structural shifts could affect the performance of a system incorporating such interfaces.

Recent and related experimental work on the relaxation of silica glass thin films in the presence of water using FTIR spectroscopy has been reported [37]. Upon aging in humid atmosphere, the films displayed shifts in their IR spectra indicative of network relaxation via incorporation of hydroxyl groups. Most pertinent to the present study, specific features of the IR spectra shift were attributed to a decrease in siloxane bond angles in the region of  $130^\circ$  and an increase in the region of  $150^\circ$ . Such a shift was not observed when these films were aged in a dry atmosphere. These experimental results indicate behavior which is similar to that which was observed in the present simulations. It is encouraging that these simulations concur well with these results; the potential model utilized herein has also produced similar behavior in previous studies [23]. These results additionally indicate that the effect observed experimentally and in the simulations may be more prevalent on surfaces that have been subjected to low

levels of surface compression associated with interface formation or processing of glass samples.

## 5. Conclusion

MD simulations of the reaction of water with silica glass surfaces before and after stress modification has given evidence that a less stable surface in the presence of water exists after stress modification. Stress modification increases the number of siloxane bond angle sites that break bonds when exposed to water. A portion of these sites are seen to be thermally stable when surfaces are heated in the absence of water. Furthermore, data presented indicate that the hydroxyl concentrations on silica glass surfaces after a compression are greater than that seen on the same surfaces prior to this stress modification.

## Acknowledgements

The authors would like to acknowledge support from DOE OBES DMS #DE-FG05-88ER45368. E. Webb would also like to acknowledge support from a Corning Fellowship.

## References

- [1] H.H. Dunken, in: M. Tomazowa, R.H. Doremus (Eds.), *Glass Surfaces*, Academic Press, New York, 1982.
- [2] R.S. McDonald, *J. Phys. Chem.* 62 (1958) 1168.
- [3] J.B. Peri, *J. Phys. Chem.* 70 (1966) 2937.
- [4] G. Hochstrasser, J.F. Antonini, *Surf. Sci.* 32 (1972) 644.
- [5] B.A. Morrow, I.A. Cody, *J. Phys. Chem.* 80 (1976) 1998.
- [6] D. Michel, V.B. Kazansky, V.M. Andreev, *Surf. Sci.* 72 (1978) 342.
- [7] C.P. Pantano, J.F. Kelso, M.J. Suscavage, in: D.R. Rossington, R.A. Condrate, R.L. Snyder (Eds.), *Surface Studies of Multicomponent Silicate Glasses: Quantitative Analysis, Sputtering Effects and the Atomic Arrangement*, Plenum, New York, 1983.
- [8] S.P. Zhdanov, L.S. Kosheleva, T.I. Titova, *Langmuir* 3 (1987) 960.
- [9] L.T. Zhuravlev, *Langmuir* 3 (1987) 316.
- [10] B.A. Morrow, I.D. Gay, *J. Phys. Chem.* 92 (1988) 5569.
- [11] R. Caracciolo, S.H. Garofalini, *J. Am. Ceram. Soc.* 71 (1988) C346.
- [12] B. Bunker, D. Haaland, T. Michalske, W. Smith, *Surf. Sci.* 222 (1989) 95.

- [13] A. Burneau, O. Barres, J.P. Gallas, J.C. Lavalley, *Langmuir* 6 (1990) 1364.
- [14] C.J. Brinker, R.K. Brow, D.R. Tallant, R.J. Kirkpatrick, *J. Non-Cryst. Solids* 120 (1990) 26.
- [15] G.I. Rudd, S.H. Garofalini, D.A. Hensley, C.M. Mate, *J. Am. Ceram. Soc.* 76 (1993) 2555.
- [16] L.R. Pal'tiel', T.M. Burkat, D.P. Dobychn, *Glass Phys. Chem.* 21 (1995) 13.
- [17] I. Chuang, G.E. Maciel, *J. Am. Chem. Soc.* 118 (1996) 401.
- [18] W. Han, M. Tomozawa, *J. Non-Cryst. Sol.* 127 (1991) 97.
- [19] D.C. Athanasopoulos, S.H. Garofalini, *J. Chem. Phys.* 97 (1992) 3775.
- [20] E.B. Webb III, S.H. Garofalini, *J. Chem. Phys.* 101 (1994) 10101.
- [21] G.V. Gibbs, E.P. Meagher, M.D. Newton, D.K. Swanson, in: M. O'Keeffe, A. Navrotsky (Eds.), *A Comparison of Experimental and Theoretical Bond Length and Angle Variations for Minerals, Inorganic Solids, and Molecules*, Academic Press, New York, 1981.
- [22] S.H. Garofalini, *SPIE Trans.* 1324 (1990) 131.
- [23] B.P. Feuston, S.H. Garofalini, *J. Appl. Phys.* 68 (1990) 4830.
- [24] S.H. Garofalini, *J. Non-Cryst. Solids* 120 (1990) 1.
- [25] B.P. Feuston, S.H. Garofalini, *J. Chem. Phys.* 89 (1988) 5818.
- [26] F. Stillinger, A. Rahman, *J. Chem. Phys.* 68 (1978) 666.
- [27] B.F. Feuston, S.H. Garofalini, *J. Phys. Chem.* 94 (1990) 5351.
- [28] J. Sauer, *Chem. Phys. Lett.* 97 (1983) 275.
- [29] J. Sauer, *J. Phys. Chem.* 91 (1987) 2315.
- [30] J. Sauer, *Chem. Rev.* 89 (1989) 199.
- [31] A.H. Narten, *J. Chem. Phys.* 56 (1972) 5861.
- [32] A. Soper, R. Silver, *Phys. Rev. Lett.* 49 (1982) 471.
- [33] B.F. Feuston, S.H. Garofalini, *Chem. Phys. Lett.* 170 (1990) 264.
- [34] S.H. Garofalini, G. Martin, *J. Phys. Chem.* 98 (1994) 1311.
- [35] G.E. Martin, S.H. Garofalini, *J. Non-Cryst. Sol.* 171 (1994) 68.
- [36] A. Nordsieck, *Math. Comput.* 16 (1962) 22.
- [37] E.G. Parada, P. Gonzalez, J. Pou, J. Serra, D. Fernandez, B. Leon, M. Perez Amor, *J. Vac. Sci. Technol. A* 14 (1996) 436.